Article:

Yu, H, Ikonic, Z, Indjin, D et al. (1 more author) (2022) The effect of interface roughness on spectral efficiency of thermophotovoltaics with multi-layer filters. Optik, 257. 168663. ISSN 0030-4026

https://doi.org/10.1016/j.ijleo.2022.168663

The effect of interface roughness on spectral efficiency of thermophotovoltaics with multi-layer filters

Hang Yu*, Z Ikonic, D Indjin and RW Kelsall

[a]School of Electronic and Electrical Engineering, University of Leeds, Woodhouse Lane, Leeds, LS2 9JT, United Kindom

ARTICLE INFO

Keywords:
interface roughness
spectral efficiency
thermophotovoltaics
Transfer matrix method

ABSTRACT

Spectral efficiency is an important parameter to characterize the optical performance of optical filters in thermophotovoltaic systems. The multilayer filters are normally designed by assuming ideally flat interfaces, but realistic structures have a degree of interface roughness present. This work explores the influence of interface roughness on the spectral efficiency, with examples including structures with different materials or number of layers.

1. Introduction

Thermophotovoltaics (TPV) convert high-grade thermal energy into electricity [1]. This approach is important in the energy industry due to its environmentally-friendly characteristics, far better than that of traditional fossil fuel energy. In 1996, JX Crystals from United States reported a portable small-scale thermophotovoltaic power generation system based on GaSb cells, with 90% total energy utilization rate [2]. Western Washington University has developed a sample of a thermophotovoltaic powered automobile, equipped with 8 GaSb TPV components and able to reach 100 miles per hour [3]. The energy conversion efficiency can be improved by optimization of PV cell bandgaps, by careful structural design of system components, and by tailoring the radiation spectrum coming to the PV cells [4]. To recycle the photons which cannot be used by PV cells, multi-layer spectral filters are used, and this paper considers the limitations coming from imperfections in practical realization of these filters, and their optimisation. The design of a spectrally selective filter based on one-dimensional photonic crystal structure has been investigated with the aim of improving the performance of thermo-photovoltaic devices [5, 6]. Using an optical filter helps to reflect back those wavelengths which lie outside the most favourable wavelength range, in order to avoid PV cell heating that leads to lower PV efficiency. Previous research has indicated that the efficiency of a TPV system can be enhanced by 45%-75% by incorporation of such filters [7]. Various filter designs, based on multi-layer stacks, have been considered in the literature, assuming that the interfaces are perfectly flat. In this work we account for the effect of interface roughness, which is known to affect the spectral properties of thin films, as discussed by A. Tikhonravov, et al [8]. We analyze its influence on the spectral efficiency of TPV systems, in particular those using multi-layer filters based on Si/SiO2 and SiO2/TiO2.

2. Theory

2.1. Transfer Matrix Method

To calculate the transmission/reflection coefficient of a multi-layer structure we use the Transfer Matrix Method [9]. The field components of outgoing and incident electromagnetic waves are related via the transfer matrix. This is calculated from interface matrices and layer matrices for the structure [10, 11]. The interface matrix is:

$$I_{ij} = \frac{1}{t_{ij}} \begin{bmatrix} 1 & r_{ij} \\ r_{ij} & 1 \end{bmatrix}, \tag{1}$$

*Corresponding author
el16hy@leeds.ac.uk (H. Yu)
ORCID(s):

where r_{ij} and t_{ij} are reflection and transmission coefficients of interface ij, respectively, themselves derived from Fresnel equations. For TE modes, r_{ij} and t_{ij} are:

$$\begin{cases} r_{ij} = \frac{q_i - q_j}{q_i + q_j} \\ t_{ij} = \frac{2q_i}{q_i + q_j} \end{cases} \tag{2}$$

and for TM modes they are:

$$\begin{cases} r_{ij} = \frac{\widetilde{n}_j^2 q_i - \widetilde{n}_i^2 q_j}{\widetilde{n}_j^2 q_i + \widetilde{n}_i^2 q_j} \\ t_{ij} = \frac{2\widetilde{n}_i^2 \widetilde{n}_j^2 q_i}{\widetilde{n}_j^2 q_i + \widetilde{n}_i^2 q_j} \end{cases}, \tag{3}$$

where q_i is the optical admittance of layer i:

$$q_i = \sqrt{\widetilde{n}_i^2 - \eta_0^2 sin\phi_0}, \tag{4}$$

where $\widetilde{n}_i$ is the refractive index of layer i, η_0 is the refractive index of air ($\eta_0 = 1$) and ϕ_0 is the incidence angle [12, 13]. For non-absorbing medium, the transfer matrix through the medium only changes the phase of the propagating wave, so it can be written as:

$$L_i = \begin{bmatrix} e^{-i\xi_i d_i} & 0 \\ 0 & e^{i\xi_i d_i} \end{bmatrix}, \tag{5}$$

where $\xi_i d_i$ is layer phase thickness, which gives the phase change of electromagnetic wave transmission through layer i. Here, $\xi_i = 2\pi q_i/\lambda$. With all the interface and layer matrices set, the total system transfer matrix S can be obtained as:

$$S = \begin{bmatrix} S_{11} & S_{12} \\ S_{21} & S_{22} \end{bmatrix} = \left(\prod_{n=1}^{m} I_{n(n-1)} L_n \right) \bullet I_{m(m+1))} \tag{6}$$

Finally, the total amplitude reflection and transmission coefficients r and t for light coming from the left are [14]:

$$\begin{cases} r = \frac{E_0^-}{E_0^+} = \frac{S_{21}}{S_{11}} \\ t = \frac{E_{M+1}^+}{E_0^+} = \frac{1}{S_{11}} \end{cases} \tag{7}$$

2.2. Effects of interface roughness

The above expressions are valid for perfectly flat multi-layer structures. In reality, the thin films cannot be perfectly flat due to limitations of growth techniques. Thus, interface roughness should be included to achieve a more realistic model. With interface roughness present, for non-absorbing media:

$$\begin{cases} r_{ij} = -r_{ji} \\ t_{ij} t_{ji} - r_{ij} r_{ji} = 1 \end{cases}, \tag{8}$$

and Eq. (1) is written as:

$$I_{ij} = \frac{1}{t_{ij}} \begin{bmatrix} 1 & -r_{ji} \\ r_{ij} & t_{ij} t_{ji} - r_{ij} r_{ji} \end{bmatrix}, \tag{9}$$

where r_{ji} and t_{ji} are the complex Fresnel reflection and transmission coefficients at interface ji, initially calculated from Eq. (2), but then modified to include the effects of roughness. The modified coefficients at the ij-th rough interface, with a random Gaussian distribution of interface height, with the root mean square denoted as Z, are [11]:

$$\begin{cases} r_{ij} = r_{ij}^0 exp[-2(sn_m\sigma)^2] \\ r_{ji} = r_{ji}^0 exp[-2(sn_{m+1}\sigma)^2] \\ t_{ij} = t_{ij}^0 exp[-\frac{(s\sigma)^2 (n_{m+1} - n_m)^2}{2}] \\ t_{ji} = t_{ji}^0 exp[-\frac{(s\sigma)^2 (n_m - n_{m+1})^2}{2}] \end{cases} \tag{10}$$

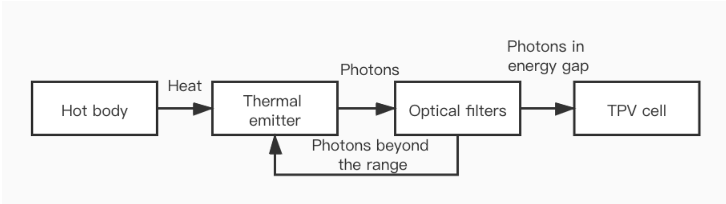

Figure 1: Diagram of TPV system

Here, the superscript 0 denotes the reflection or transmission coefficients for an ideal interface,$\sigma = 1/\lambda$, and $s = 2\pi Z$.

2.3. Spectral efficiency

The spectral efficiency of an optical filter is the ratio of the energy that can be absorbed by the PV cell and the total energy entering the filter [15], and is a measure of the performance of the filter used in the TPV system. In this section, the simulation model is briefly described. The multi-layer structure, as shown in Fig. 1, acting as the optical filter is located between the hot body (in this case, black body) and the TPV cell (in our calculations a GaSb cell). The radiation power P_{rad} which is received by the GaSb cell can be expressed as:

$$\begin{aligned} P_{Rad} &= P_{Tot} - P_{Ref} \\ &= \int_0^\infty \frac{n_{BB}^2 \omega^3 \hbar}{4\pi^2 c^2 exp\left(\frac{\hbar\omega}{kT_{BB}}\right) - 1} \bar{T}_{BC}(\omega)\, d\omega - \int_{\omega_{gap}}^\infty \frac{n_{PV}^2 \omega^3 \hbar}{4\pi^2 c^2 exp\left(\frac{\hbar\omega - eV}{kT_{PV}}\right) - 1} \bar{T}_{CB}(\omega)\, d\omega \end{aligned} \tag{11}$$

where $\overline{T_{BC}}(\omega)$ is the transmittance from the black body to the cell, and is given by

$$\overline{T_{BC}}(\omega) = \int_0^{\theta_X} \left\{ T_{BC\_TE}(\omega,\theta) + T_{BC\_TM}(\omega,\theta) \right\} \cos(\theta)\sin(\theta)\, \mathrm{d}\,\theta \tag{12}$$

Similarly, the expression for $\overline{T_{CB}}(\omega)$), which is the transmittance from cell to black body is:

$$\overline{T_{CB}}(\omega) = \int_0^{\theta_X} \left\{ T_{CB\_TE}(\omega,\theta) + T_{CB\_TM}(\omega,\theta) \right\} \cos(\theta)\sin(\theta)\, \mathrm{d}\,\theta \tag{13}$$

The power generated by the TPV system equals the photon flux from black body to the cell minus the part which is reflected back to the black body:

$$P_{Gen} = eV \left(\int_{\omega_{gap}}^\infty \frac{n_{BB}^2 \omega^2}{4\pi^2 c^2 exp\left(\frac{\hbar\omega}{kT_{BB}}\right) - 1} \bar{T}_{BC}(\omega)\, d\omega - \int_{\omega_{gap}}^\infty \frac{n_{PV}^2 \omega^2}{4\pi^2 c^2 exp\left(\frac{\hbar\omega - eV}{kT_{PV}}\right) - 1} \bar{T}_{CB}(\omega)\, d\omega \right\} \tag{14}$$

The system efficiency η_{sys} can be obtained as P_{rad} divided by P_{gen} [16, 17]. To calculate the spectral efficiency, it is assumed that all the power transmitted to the cell with larger photon energy than the bandgap of GaSb cell (i.e. $0.7eV$) can be converted to electricity, so the transmittance of these photons will ideally be 1. All other photons should be reflected back to the emitter, i.e. the transmittance for them will ideally be 0. The expression for the spectral efficiency can then be written as:

$$\eta_{Spe} = \frac{\int_{\omega_{gap}}^\infty \frac{n_{BB}{}^2 \omega^3 \hbar}{4\pi^2 c^2 exp\left(\frac{\hbar\omega}{kT_{BB}}\right) - 1} \bar{T}_{BC}(\omega)\, d\omega}{\int_0^\infty \frac{n_{BB}{}^2 \omega^3 \hbar}{4\pi^2 c^2 exp\left(\frac{\hbar\omega}{kT_{BB}}\right) - 1} (1 - \bar{R}_{BC})(\omega)\, d\omega} \tag{15}$$

In numerical calculations the limits of the integrals were approximated, with 0 and infinity replaced by frequencies corresponding to wavelengths of $6\mu m$ and $0.5\mu m$ respectively.

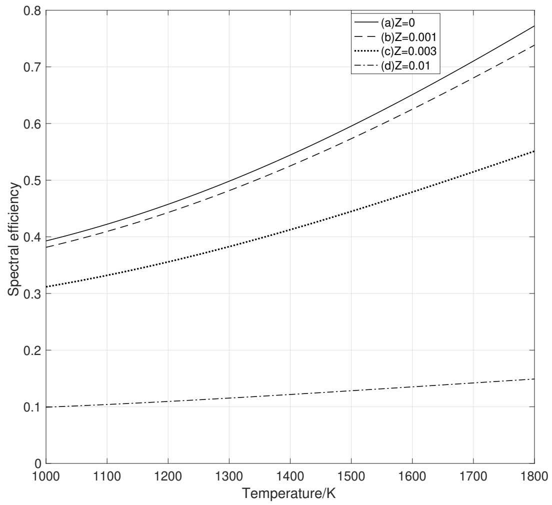

Figure 2: $(LH)_5$ structure of MgF_2/Ge with (a) perfectly flat interfaces, Z=0 (b) Z=0.001μm (c) Z=0.003μm (d) Z=0.01μm.

3. Results and discussion

Since the spectral efficiency is one of the most important parameters which define the optical performance of a TPV system, we considered the effect of interface roughness on spectral efficiency. Firstly we considered the filter structure proposed in [18], comprising MgF_2 and Ge layers, with refractive indices of 1.36 and 4.2 respectively. In the initial periodic structure, with no layer thickness optimization, the widths of low and high index layers were 0.495 and 0.16μm. In this case, the MgF_2 and Ge array is $(LH)_5$. A black body temperature range of 1000-1800 K was considered. Fig. 2 shows the spectral efficiency variation when changing the rms roughness height Z.

Introducing finite Z clearly has a strong influence on the spectral efficiency of this structure. For Z = 0.001μm, the efficiency decreases only mildly, from 39-77% to 38- 74% in the temperature range 1000-1800K; however, when Z was increased to 0.01μm, the efficiency decreases considerably, to just 10– 15%. Fig. 3 shows the impact of interface roughness on the spectral efficiency for an alternative filter – a 10-layer Si/SiO_2 array with a $L/2H(LH)_4$ structure [16]. The key difference from the previous example is the aperiodicity in the initial layers.

The interface roughness seriously degrades the spectral efficiency in this structure, too. The curves show a moderate decrease - from 12- 59% to 11- 56% in the temperature range 1000-1800K when the rms roughness height is 0.001μm, and a very significant reduction, to 1 – 3%, when Z = 0.01μm.

Fig. 5 shows the spectral efficiency for a 10 layer, SiO_2/Si periodic $(LH)_5$ filter structure. This choice is based on comparison of results shown in Fig. 4. The reflectance in the bandgap region steeply increases to 99% when the number of periods increased from 4 to 8. The reflectance reaches 100% for 10-layer structure. Therefore, the 10-layer periodic array of Silicon and SiO_2 is chosen as the initial model, in which the roughness is introduced. From Fig. 5, for Z=0.001μm the spectral efficiency only slightly decreases relative to the case of perfectly flat layers, from 19- 61% to 18- 55%, but for Z=0.01μm the spectral efficiency dramatically decreases to 1- 4%. When the high index material is changed to from Si to TiO_2, the spectral efficiency changes from 19- 56% for flat interfaces to 18- 53% for Z =0.001μm, and 1 – 3% for Z = 0.01μm (Fig. 6). If no spectral filter is used, the efficiency is only 12-40%, as given by line (e) in Fig. 5.

In summary, these calculations indicate that the tolerable level of rms interface roughness is 0.001-0.003μm, with Z = 0.01μm being highly detrimental to filter performance. All the above examples involved 10-layer stacks. To obtain a better spectral efficiency, the number of layers and their thicknesses may be optimized as well. For multi-layer structures composed of SiO_2 and TiO_2, the spectral efficiency of 10-layer, 8-layer and 6-layer stacks are compared in Fig. 7. In the presence of interface roughness, the 6-layer structure shows higher efficiency than 10-layer and 8-layer structures,

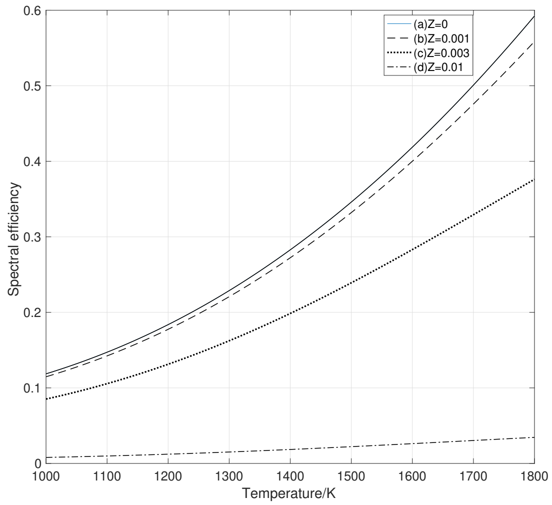

Figure 3: Spectral efficiency of an $L/2H(LH)_4$ structure of Si/SiO_2 with (a) perfectly flat interfaces, Z=0 [16], (b) Z=0.001μm (c) Z=0.003μm (d) Z=0.01μm. n(Si) and n(SiO_2) are 3.4 and 1.5, and d(Si)=0.17μm, d(SiO_2)=0.39μm.

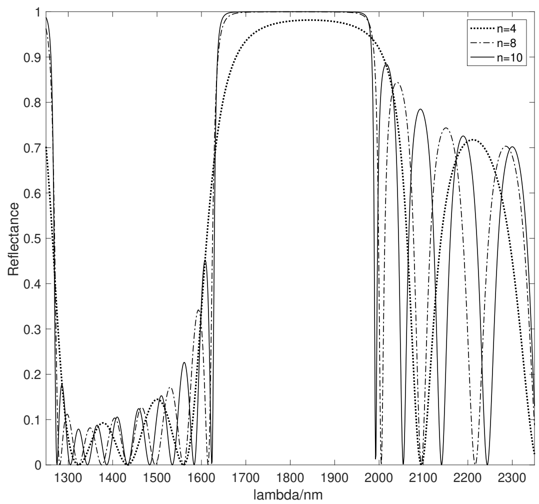

Figure 4: Reflectance of Si/SiO_2 $(LH)_n$ structures with (a) n=4 (b) n=8 (c) n=10. The refractive indices n(Si) and n(SiO_2) are 3.97 and 1.45, and widths d(Si)=30.18nm, d(SiO_2)=82.76nm.

indicating that, if appreciable interface roughness cannot be avoided in practice, 6-layer structures would be the best choice in terms of optical performance.

In another example the layer thicknesses of the Si/SiO2 structure were optimized using genetic algorithm. A fitness function was set, having the filter layer thicknesses as independent variables, to determine if each "chromosome" was better than its "father" generation [17, 19]. The target function for the nth generation can be written as:

$$T' = \sqrt{\frac{1}{n}\sum_{i=1}^{n}\left(T_e\left(\lambda_i, d\right) - T(\lambda_i, d)\right)^2} \tag{16}$$

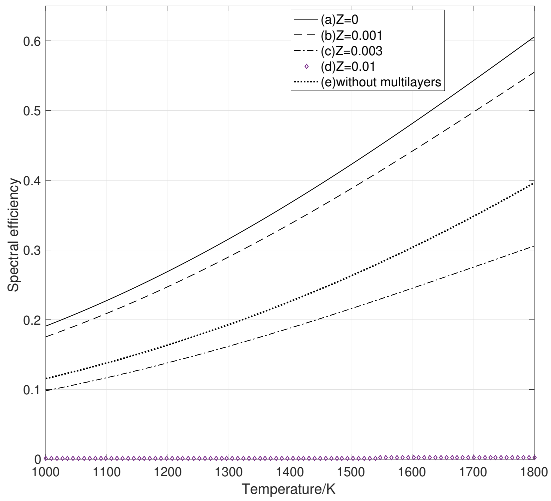

Figure 5: $(LH)_5$ structure of Si/SiO_2 with (a) Z=0 (b) Z=0.001μm (c) Z=0.003μm (d) Z=0.01μm (e) without multilayer filter. n(Si) and n(SiO_2) are 3.97 and 1.45, and d(Si)=30.18nm, d(SiO_2)=82.76nm.

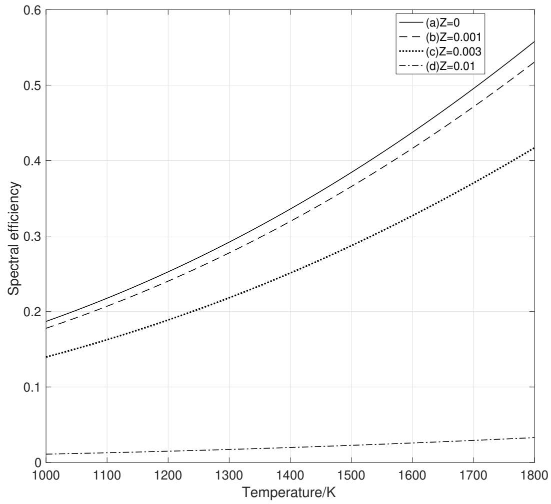

Figure 6: $(LH)_5$ structure of SiO_2/TiO_2 with (a) Z=0 (b) Z=0.001μm (c) Z=0.003μm (d) Z=0.01μm. n(TiO_2) is 2.1 and d(TiO_2)=57.14nm.

where $T(\lambda_i, d)$ is the calculated transmittance and T_e can be taken as 1 for photon energies higher than the PV cell band gap, and 0 otherwise [15, 20]. This function is designed to find the difference between calculated and target values. The overall, global target is to minimize T'. A structure optimized in this way does not necessarily yield the global maximum, but it can be expected that it will identify a design which lies close to the top of the performance range. Alternatively, the spectral efficiency can be used as the optimization target function (and this then depends on the black body source temperature).

Table 1 lists the optimum thicknesses of each layer obtained both by using transmittance T' as the target (GA_T entries) and by using spectral efficiency at T = 1500K as the target (GA_{SE} entries). Some of layer thicknesses have been modified significantly by the evolution algorithm. Fig. 8 compares the spectral efficiencies of structures optimized by both the above methods with the unoptimized structure, throughout the temperature range 1000-1800K. The optimized

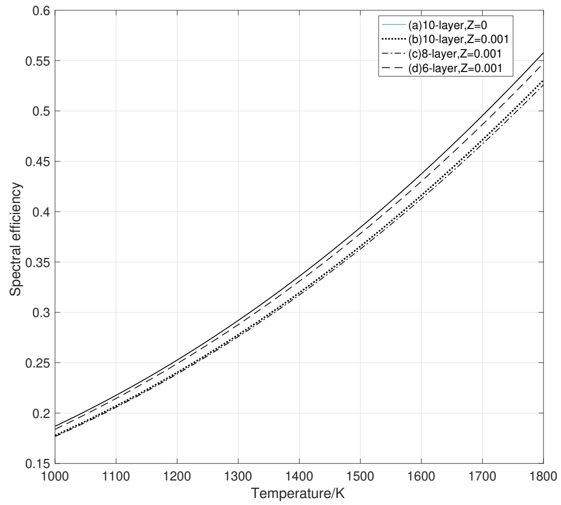

Figure 7: $(LH)_5$ structure of SiO_2/TiO_2 with (a) perfectly flat 10-layers (b) 10-layers, Z=0.001μm (c) 8-layers, Z=0.001μm. (d) 6-layers, Z=0.001μm.

Table 1
Optimized $(LH)_5$ Si/SiO_2 structures layer thicknesses. n(high)=3.9766, n(low)=1.4585.

	L	H	L	H	L	H	L	H	L	H
Original/nm	82.276	30.174	82.276	30.174	82.276	30.174	82.276	30.174	82.276	30.174
GA_T/nm	72.283	2.8288	8.3107	26.968	77.4558	27.5338	75.7936	27.7224	81.4449	0.3772
GA_{SE}/nm	70.7242	2.9044	8.3189	26.577	73.8153	25.0146	73.3876	26.8928	72.6942	0.4046

structures have higher spectral efficiencies than the original structure for most of the temperature range considered, both with and without interface roughness included. Use of the spectral efficiency target results in designs with better performance at low temperatures, but the transmittance target yields designs which perform better at the higher end of the temperature range.

4. Conclusion

Using the Transfer Matrix method, the effects of interface roughness on the spectral efficiency of multi-layer structures used as filters in TPV systems are investigated. Different materials and structures are tested in this respect, both from other published research or our own designs, based on which the guidelines for tolerable interface roughness in these structures were given, in the range Z=0.001μm to Z=0.003μm. Also, if the roughness cannot be avoided, the structures with smaller number of layers are generally preferable. Finally, the optimization of layer thicknesses with interface roughness accounted for can slightly improve the optical performance of a filter, but it is still below that with no roughness present.

References

[1] C. Ferrari, F. Melino, M. Pinelli, P. R. Spina, M. Venturini, Overview and status of thermophotovoltaic systems, Energy Procedia 45 (2014) 160–169.

[2] J. Crystals, Jx crystals – infrared energy, `https://jxcrystals.com/wp/`, accessed 14 May 2021.

[3] S. Christ, M. Seal, Viking 29 – a thermophotovoltaic hybrid vehicle designed and built at western washington university, `https://doi.org/10.4271/972650.`, accessed 14 May 2021.

[4] F. K. Khosroshahi, H. Ertürk, M. P. Mengüç, Optimization of spectrally selective si/sio2 based filters for thermophotovoltaic devices, Journal of Quantitative Spectroscopy and Radiative Transfer 197 (2017) 123–131.

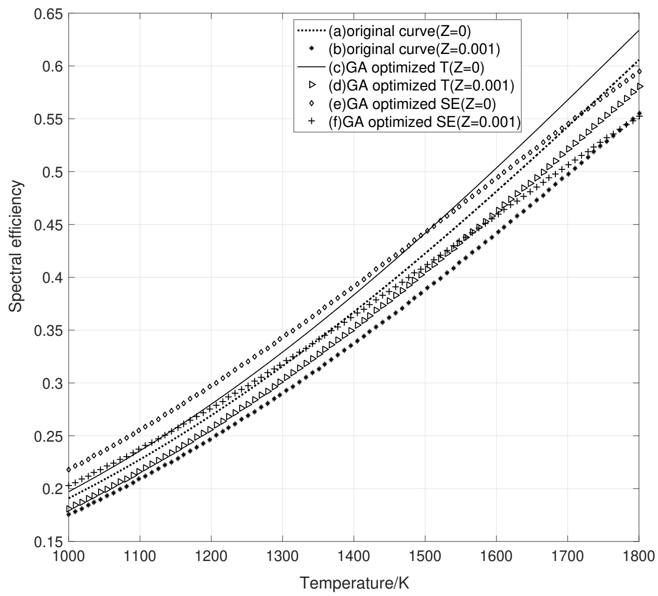

Figure 8: The spectral efficiency of $(LH)_5$ structure with Si/SiO_2 with (a) original 10-layer periodic structure with Z=0, (b) original 10-layer periodic structure with Z=0.001μm, (c) optimized for Transmittance, with Z=0, (d) optimized for Transmittance, with Z=0.001μm, (e) optimized for Spectral efficiency, with Z=0, (f) optimized for Spectral efficiency, with Z=0.001μm.

[5] A. Ghanekar, M. Sun, Z. Zhang, Y. Zheng, Optimal design of wavelength selective thermal emitter for thermophotovoltaic applications, Journal of thermal science and engineering applications 10 (1).
[6] S. An, G. Yingjun, Filter characteristics of one-dimensional photonic crystal with complex dielectric constant, Chinese Journal of Lasers 36 (6) (2009) 1535.
[7] E. Yablonovitch, Inhibited spontaneous emission in solid-state physics and electronics, Physical review letters 58 (20) (1987) 2059.
[8] A. V. Tikhonravov, M. K. Trubetskov, A. A. Tikhonravov, A. Duparre, Effects of interface roughness on the spectral properties of thin films and multilayers, Applied optics 42 (25) (2003) 5140–5148.
[9] L. A. Pettersson, L. S. Roman, O. Inganäs, Modeling photocurrent action spectra of photovoltaic devices based on organic thin films, Journal of Applied Physics 86 (1) (1999) 487–496.
[10] T. Zhan, X. Shi, Y. Dai, X. Liu, J. Zi, Transfer matrix method for optics in graphene layers, Journal of Physics: Condensed Matter 25 (21) (2013) 215301.
[11] C. C. Katsidis, D. I. Siapkas, General transfer-matrix method for optical multilayer systems with coherent, partially coherent, and incoherent interference, Applied optics 41 (19) (2002) 3978–3987.
[12] I. H. Malitson, Interspecimen comparison of the refractive index of fused silica, Josa 55 (10) (1965) 1205–1209.
[13] C. Tan, Determination of refractive index of silica glass for infrared wavelengths by ir spectroscopy, Journal of Non-Crystalline Solids 223 (1-2) (1998) 158–163.
[14] H. Hardhienata, A. I. Aziz, D. Rahmawati, H. Alatas, Transmission characteristics of a 1d photonic crystal sandwiched by two graphene layers, in: Journal of Physics: Conference Series, Vol. 1057, IOP Publishing, 2018, p. 012003.
[15] B. Chaudhuri, G. Garai, Grid clustering with genetic algorithm and tabu search process, Journal of Pattern Recognition Research 4 (1) (2009) 152–168.
[16] F. O'Sullivan, I. Celanovic, N. Jovanovic, J. Kassakian, S. Akiyama, K. Wada, Optical characteristics of one-dimensional si/ si o 2 photonic crystals for thermophotovoltaic applications, Journal of Applied Physics 97 (3) (2005) 033529.
[17] R. Musin, A. Zheltikov, Designing dispersion-compensating photonic-crystal fibers using a genetic algorithm, Optics communications 281 (4) (2008) 567–572.
[18] K. Binidra, R. Miloua, M. Khadraoui, Z. Kebbab, A. Bouzidi, N. Benramdane, Spectral control in thermophotovoltaic systems by optimized one-dimensional photonic crystals, Optik 156 (2018) 879–885.
[19] J.-H. Lu, D.-P. Cai, Y.-L. Tsai, C.-C. Chen, C.-E. Lin, T.-J. Yen, Genetic algorithms optimization of photonic crystal fibers for half diffraction angle reduction of output beam, Optics express 22 (19) (2014) 22590–22597.
[20] Y. Wang, S. Gao, H. Zhang, Z. Tang, An improved genetic algorithm based complex-valued encoding, IJCSNS Int. J. Computer Science and Network Security 10 (6) (2010) 168–174.